Gravity: Jurnal Ilmiah Penelitian dan Pembelajaran Fisika

http://jurnal.untirta.ac.id/index.php/Weight force

ISSN: 244-515x; e-ISSN: 2528-1976

Vol. 10, No. 1, April 2024, Page 38 - 53

Identification of regional rock depth-residual gravity anomaly based on spectrum analysis of geothermal prospect area of Wayratai Lampung

Syamsurijal Rasimeng, Ilham Dani, Widya Putri Syahranti*, Ivana Jayarani Sitompul, Fadhil Muhammad Nizam

Department of Geophysical Engineering, Universitas Lampung, Indonesia

**E-mail: widya.putri21@students.unila.ac.id*

(Received: 21 December 2023; Accepted: 28 April 2024; Published: 29 April 2024)

ABSTRAK

The weight force method is a geophysical method that is sensitive to vertical changes, therefore this method is favored for studying intrusion contacts, bedrock, geological structures, ancient river deposits, holes in the rock mass, buried shaff, and others. The location of the research area is in the Way Ratai geothermal area, Padang Cermin District, Pesawaran Regency, Lampung Province. This research aims to determine the depth of regional and residual anomalies and to identify weight force anomalies based on 2-dimensional subsurface conditions. Five passes were sliced, namely A-A', B-B', C-C', D-D', and E-E' on the complete Bouguer anomaly cross section, and the resulting values of regional depth, residual, wavelength, and cutoff value as the boundary of the intersection between regional and residual anomalies. The complete Bouguer anomaly values range from 54 mGal to 100 mGal, the regional anomaly is 56 mGal to 90 mGal, and the residual anomaly is 19 mGal to 4 mGal. The depth of the regional anomaly is 5219.4m and the residual anomaly is at a depth of 336.77m.

Keywords: Regional, residual, wayratai, weight force

DOI: 10.30870/gravity.v10i1.23575

INTRODUCTION

Indonesia is ranked as the country with the largest geothermal potential in the world, with this energy potential spread across 285 locations along volcanic areas. Some of the areas that contribute to the geothermal potential include Mount Lawu in West Java, Ciwidey Crater in the Mount Patuha area, Umbul Temple in Central Java, Air Kelinsar geothermal field in South Sumatra, Way Selabung geothermal in South Ogan Komering Ulu, and Batu Bini in South Kalimantan (Hakim *et al*., 2022). Lampung Province is also an area that has significant

geothermal energy reserve potential in Indonesia. This is due to the volcanic path that crosses Lampung, which is part of the Mediterranean circumpolar mountain range. One of the geothermal potentials that has not been fully explored in Lampung Province is Way Ratai (Putri *et al*., 2014).

Geothermal exploration is emerging as a solution to the challenge of rising non-renewable energy scarcity as energy demand grows. Geothermal utilization offers various advantages over the use of fossil fuels. Geothermal can be a renewable energy alternative that remains available, independent of weather conditions or seasons (Nurwahyudin & Harmoko, 2020). Law No. 27 Year 2003 emphasizes that thermal energy sources in the form of hot water, water vapor, rocks, minerals, and gas are considered a geothermal system that cannot be separated genetically. Indonesia has a wide distribution of geothermal energy, with more than 300 geothermal resource points spread from Sabang to Merauke. Geothermal energy can act as a substitute for non-renewable energy sources, such as fossil fuels, for power generation and transportation purposes. Some of the advantages of using geothermal energy are that it provides energy at a constant rate and is not dependent on weather or seasons, it can complement new and renewable energy, and it helps reduce gas emissions (Marry *et al*., 2017).

Active utilization of geothermal energy can make a significant contribution to reducing the problem of electricity availability, which is still a problem that has not been fully solved by the Government of Indonesia (Nurwahyudin & Harmoko, 2020). Geothermal energy is a form of energy obtained from the heat stored in the earth. This source of geothermal energy arises from tectonic processes that have occurred within the Earth since the formation of the planet. In addition, this heat also comes from solar radiation absorbed by the earth's surface (Fandari *et al*., 2014). Geothermal energy is a renewable primary energy source. According to data from the Indonesian Ministry of Energy and Mineral Resources (MEMR), the potential of geothermal energy in Indonesia reaches 29.5 gigawatts (GW), and this potential value is likely to continue to increase along with exploration activities. Data on geothermal energy utilization in Indonesia until 2020 reached 3,109.5 megawatts (MW) according to the National Energy General Plan 2020. This means that only about 10.5% of the geothermal energy potential has been utilized. The Indonesian government, through the Ministry of Energy and Mineral Resources, seeks to increase the utilization of new renewable energy sources by developing Geothermal Power Plants (PLTP) both through state-owned companies and by granting Geothermal Working Area (WKP) processing licenses to private companies (IPP) (Khasmadin & Harmoko, 2021).

Geologically, the study area is dominated by rock formations of young volcanic origin (Qhv), originating from both Mount Pesawaran/Ratai and Mount Betung. These rocks include lava (andesite-basalt), breccia, and tuff. The stratigraphy of Way Ratai geothermal field can be divided into four categories (Mangga *et al*., 1993). First, the Tertiary rocks consist of sedimentary rocks of the Ratai Formation, involving conglomerates, sandstones, lava breccias, and mudstones, sometimes associated with andesite tuff scattered in the south-southwest. Second, the Pre-eruption Volcanic rocks of Mount Betung and Ratai, include various types of volcanic rocks from old to young such as Gebang volcanic rocks (GV), Gebang ignimbrite rocks (GI), Gebang lava flow rocks (GL), debris deposits (ED), and Banjarmeger volcanic rocks (BV). Third, Volcanic Rock Eruptions of Mount Betung and Ratai, where Quaternary volcanic rocks erupted into two eruption sources, namely the eruption of Mount Betung and Ratai at the base of the Gebang Caldera. Fourth, Surface Deposits consist of Lava Deposits (LH) and

Alluvium Deposits (Sarkowi *et al*., 2021). The structural history of the Tanjungkarang sheet includes tectonic events from the late Paleozoic to the early Quaternary. According to the Tanjung Karang stratigraphic sequence, the Way Ratai area is located within the context of the Tertiary stratigraphic sequence and is regionally included in the Bukit Barisan Line. The Tertiary rocks revealed in the Tanjung Karang sheet consist of collapsed volcanic continental arc rocks and sediments that were deposited together extensively namely the Sabu, Campang, and Tarahan Formations. The three formations span from the Paleocene to early Oligocene periods (Zaenudin *et al*., 2011).

The morphology of Way Ratai and its surroundings has been classified into seven morphological units, which include lava domes, coarse-textured hills, fine-textured hills, old hills, weakly undulating plains, gentle plains, and isolated hills (Mangga *et al*., 1993). Way Ratai Geothermal Field is located in a volcanic complex environment consisting of two adjacent volcanic cones, namely Mount Ratai in the southwest and Mount Betung in the northeast. The formation of the geothermal system in Way Ratai was influenced by the formation of the landscape of the volcanic complex, which occurred during the Quaternary period and was influenced by endogenous and exogenous factors. Endogenous factors include the dynamics of the Ratai and Betung Volcanoes, as well as regional tectonic movements or faults that affect the Way Ratai geothermal area. On the other hand, exogenous factors are related to hydrophysical processes, in which erosion of the earth's surface plays an important role. These two natural processes eventually form landforms such as plains and hills. Landforms in the Way Ratai geothermal area are categorized based on their characteristics, including morphology, slope, texture, and river flow patterns (Donovan *et al*., 2020).

Some related studies are research by Putri *et al*. (2014), which focused on the Way Ratai geothermal system and classified it as a liquid-phase dominated system with a water source originating from the highlands. Its methods included geochemical analysis and thermal manifestation surveys. Another study, conducted by Donovan *et al*. (2020), examined the distribution of thermal conductivity of rocks in Way Ratai geothermal field. This study concludes that the thermal conductivity value in Way Ratai geothermal field is influenced by geological factors such as faults and alignments, the presence of alteration, and hot water manifestations. Karyanto *et al*. (2020) also investigated Way Ratai's geothermal potential by conducting thermal conductivity measurements, obtaining thermal resistivity values of 1.344 to 17.527 mK/W, conductivity of 0.056 to 0.664 W/mK, and temperatures between 22.7℃ and 52.6℃. Other research by Karyanto *et al*. (2022) included numerical modeling of the Way Ratai geothermal system and concluded that the Way Ratai geothermal system can be categorized as a high enthalpy system because it has a large and thick area with high temperatures. Research by Wahyudi (2006) on the study of geothermal potential in Mount Ungaran, Central Java using the Controlled Source Audio-Frequency Magneto-telluric (CSAMT) method at a depth of 75 cm, surface temperature survey, and geochemistry with the results of the estimated geothermal potential of the study area is 11.25 mW for 5 km2.

This research aims to understand the depth of regional and residual anomalies and identify weight force anomalies based on subsurface conditions in a 2-dimensional context using weight force data. This method was chosen because weight force is considered very responsive to vertical changes, so it is often used in the study of intrusion contacts, bedrock, geological structures, ancient river deposits, holes in rock masses, and other hidden formations

(Sarkowi, 2014). The weight force measurements carried out to obtain information about the subsurface layer can be applied to analyze geological structures, subsurface layers, and faults that are potential pathways for geothermal fluid movement (Susilawati *et al*., 2023). In geothermal exploration research, the application of gravity methods allows the identification of differences in rock density in the subsurface layers that form geothermal systems (Sihombing & Rustadi, 2020). The distribution of temperature and heat energy below the Earth's surface is the source of geothermal heat. The temperature at the surface is determined by heat conduction through solid rock and convection in circulating fluids (Emujakporue, 2017). An increase in the Earth's temperature will correspond to an increase in the depth below the surface. If the Earth's temperature changes as a function of depth, it is called a geothermal gradient. A geothermal system is considered ideal if it meets several criteria, such as having a heat source that comes from plutonic rocks or magma that has been frozen. In addition, the system must have porous rocks or reservoirs, where hot water or steam is retained (Suharno, 2013). The method used to separate regional and residual anomalies is the moving average method. This method is used to solve the problem that the required anomaly results are anomalies according to the target depth while the gravity anomaly obtained is a combination of shallow and deep sources (Siombone *et al*., 2022). Gravity anomalies from sources at a certain depth have large wavelengths, while gravity anomalies from shallow sources have smaller wavelengths. Based on these characteristics, it is possible to separate effects originating from shallow depths (Zuhdi *et al*., 2019).

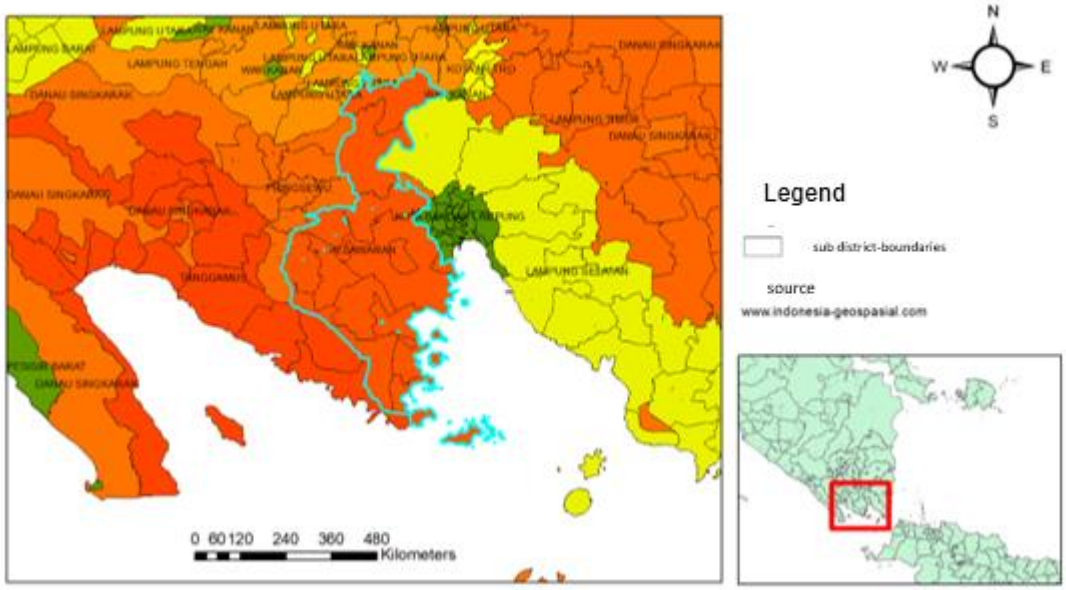

Figure 1. Administrative map of the study area

RESEARCH METHODS

This research was conducted at the location of Way Ratai, Lampung, using the aerial data collection method and using the administrative map listed in Figure 1. The data used in this study are gravity data related to the density and density of rock masses against their environment by utilizing gravity information from the GGMplus (Global Weight Force Model

Plus) satellite in 2013. The advantage of GGMplus data lies in its higher spatial resolution compared to other satellite gravity data, such as TOPEX and BGI (Suprianto *et al*., 2021). With a spatial resolution of 200 m, GGMplus can be used as an initial mapping tool to provide a generalized figure of an area prior to more localized primary data collection (Hirt *et al*., 2013).

The gravity method is a geophysical exploration technique that utilizes variations in gravitational acceleration at the Earth's surface as the basis for investigation. These variations occur due to small differences in the gravitational field caused by mass variations within the Earth's crust. (Sari, 2014). The basic principle on which the gravity method is based is the law of gravitational attraction between particles discovered by Newton (Telford *et al*., 1990). The gravity method is one of the most significant techniques in determining the geothermal potential of an area (Charisma *et al*., 2022). This approach allows the figuring of subsurface conditions by differentiating rock densities, enabling the identification of each component in the geothermal system, such as overburden, reservoir, and heat source. This is due to the interpretation that geothermal reservoir rocks have low density as a result of high temperature and high porosity (Raehanayati *et al*., 2013). This method is also useful for locating subsurface structures such as traps and fluid movement pathways, such as recharge areas and discharge areas, which are important factors in the formation of geothermal systems (Telford *et al*., 1990). The advantage of the gravity method lies in its ability to provide detailed information on geological structures and rock density contrasts at the initial survey stage. In the context of geothermal research, the difference in rock density is used as a guideline for gravity method research. Thus, the presence of heat sources beneath the earth's surface can produce density variations with the surrounding rock masses (Hidayat & Basid, 2011).

Spectrum analysis is performed to estimate the window width and obtain an approximate depth of the gravity anomaly. In addition, spectrum analysis can be used to compare the response spectra of different screening methods. The process of spectrum analysis involves the Fourier transform of predetermined trajectories. This Fourier transform is used to decompose or reconstruct any waveform into sine waves of varying frequencies. Spectrum analysis is run on multiple trajectories so that the average depth of the regional Bouguer anomaly can be calculated. The power spectrum of the Bouguer anomaly is calculated by transforming the Fourier gravity data into the frequency domain with the equation below (Blakely, 1995).

$$F(k) = \int_{-\infty}^{\infty} f(x) e^{-ikx} dx \quad (1)$$

Where k In the equation above is a wavenumber to a wavelength λ or frequency f, where the value is

$$k = \frac{2\pi}{\lambda} \quad (2)$$

The *Fourier* transform F(k) is generally a complex function with a real component and an imaginary component, i.e. $F(k) = \mathrm{Re}F(k) + i\mathrm{mF}(k)$, Or it can also be written as follows:

$$F(k) = |F(k)| e^{i\theta k}, \quad (3)$$

Where

$$|F(k)| = [\mathrm{Re}F((k)^2 + (\mathrm{Im}F(k))^2]^{1/2}, \quad (4)$$

$$\theta(k) = \arctan \frac{\mathrm{ImF(k)}}{\mathrm{ReF(k)}} \quad (5)$$

Function $|F(k)|$represents the amplitude and $\theta(k)$is a phase of the spectrum. Equation (2) is also known as *the power spectrum* equation.

The process of determining the depth estimation of regional and residual anomalies is carried out by analyzing the amplitude spectrum against wavenumbers k, Where the *slope* or slope of the graph shows the depth of the source of the anomaly. Based on depth, regional anomalies are deeper anomalies than residual anomalies and *noise* is shallower than residual anomalies (Supriyadi *et al*., 2019). Residual anomalies are caused by shallow anomalies that have high frequencies and short wavelengths while regional anomalies are caused by deep anomalies that have low frequencies and long wavelengths (Telford *et al*., 1990).

The same is the case with the power spectrum equation derived by (Blakely, 1995) pada a horizontal plane with height z_0 and subsurface objects with depth z', where z'>z_0.

By limiting the *Fourier transform* of the gravitational potential in a horizontal flat plane by z'=z0 And since a point of mass (equal to the part on the mass of a sphere with uniform density) located in a flat plane of the Fourier transform can be written with the equation:

$$F\left[\frac{1}{r}\right] = 2\pi \frac{e^{|k|(z_0 - z')}}{|k|} \quad (6)$$

The gravitational potential of a point of mass is given by $U = \frac{GM}{r}$ where G is the gravitational constant such that the Fourier transform can be rewritten to:

$$F(U) = GMF\left[\frac{1}{r}\right] \quad (7)$$

$$F(U) = 2\pi GM \frac{e^{|k|(z_0 - z')}}{|k|} \quad (8)$$

The gravitational acceleration g can be related to potential, following the equation $g = \nabla U$, so that each component g It is simply a derivative of U. In general, the vertical gravitational acceleration pull on a point of mass is newly derived $U = \frac{GM}{r}$ which can be written as follows:

$$g_z = GM \frac{\partial}{\partial z} \frac{1}{r} \quad (9)$$

If the observation of gravitational potential in a horizontal flat plane, then this plane can give the equation of the Fourier transform as follows:

$$A = Ce^{|k|(z_0 - z')} \quad (10)$$

Where A = amplitude

C = Constanta

The amplitude value in this case can be found using the power spectrum equation $|F(k)| = [\mathrm{Re}\, F((k)^2 + (\mathrm{Im}\, F(k))^2\,]^{1/2}$ or it can also be written as follows $A(k) = [\mathrm{Re}G((k)^2 + (\mathrm{Im}G(k))^2]^{1/2}$.

Then, by applying logarithms to the results of the *Fourier transform*, a correlation can be revealed between the amplitude of the spectrum (A) with the wavenumber (k) and the difference in anomalous depth (z_0-z'). Therefore, the relationship can be described through the following equation:

$$\ln A = (z_0 - z')|k| \tag{11}$$

By utilizing the equation mentioned above, we can identify the field boundary of an anomalous source by producing a logarithmic graph of amplitude $(z_0 - z') \ln A$ against wavenumber k. Therefore, the depth of the anomalous source boundary plane can be directly determined through the slope of the graph $(z_0 - z')\ \ln A$ towards k.

Blakely (1995) derives the spectrum of the observed gravity potential in a horizontal plane. An illustration to determine the depth by regressing the logarithmic data of the Fourier Transform results is shown in:

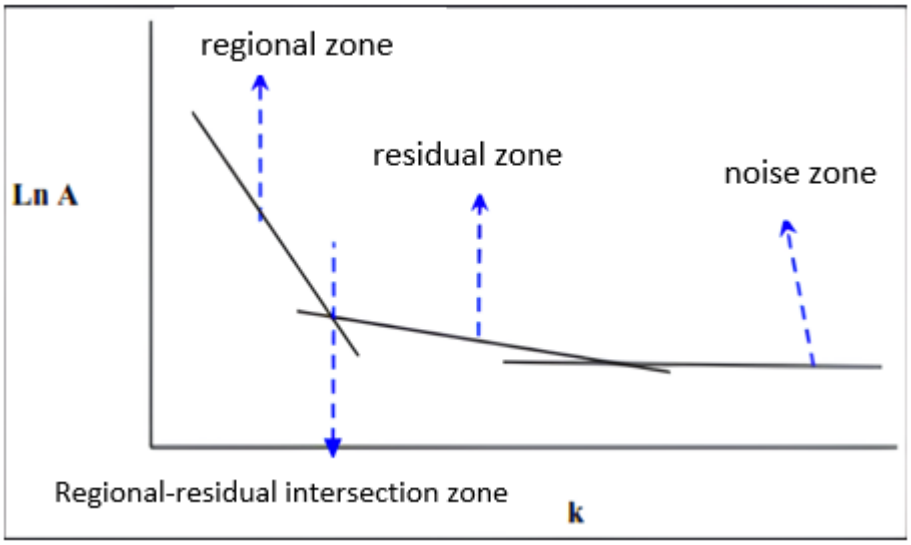

Figure 2. The curve of Ln A against K (Blakely, 1995)

Mathematically, an anomaly in the gravity field can be defined as the difference between the gravity field measured on the topography and the theoretical gravity field on the topography, at position (x, y, z). The theoretical gravity field refers to the field caused by non-geological factors, with values calculated based on theoretical formulas. The value of this field is affected by the altitude, latitude, and topographic mass around the point (Zakaria, 2021). The 4D gravity anomaly measured in the field is the total anomaly from various depths. Anomalies originating from shallow depths have small wavelengths, while anomalies originating from greater depths have larger wavelengths. By utilizing this wavelength difference, the effects from shallow depths can be separated from the anomalies originating from deep depths. The process of separating shallow effects can be done using a moving average filter (Indriana *et al*., 2018), which involves applying 2D convolution to the measured gravity data.

There are two types of modeling commonly used for data interpretation: gravity forward modeling and inversion modeling. Forward modeling, also known as forward modeling, involves elaborating data from a model by calculating the theoretical response and distribution properties of the anomalous source. In contrast, inversion modeling, also known as inversion

modeling, is used to elaborate a model from field measurement data by analyzing theoretical studies of the obtained model (Nurul *et al*., 2020). This research uses backward modeling or inverse modeling.

The research phase begins with downloading data from the GGMPlus website and then making corrections, namely latitude correction, free air correction, Bouguer correction, and terrain correction to produce a complete Bouguer anomaly value. This complete Bouguer anomaly was then sliced into 5 passes as shown in Figure 6. Terrain correction could not be done because the data from the GGMPlus website is an airborne survey. The detailed research steps are presented in the Figure below.

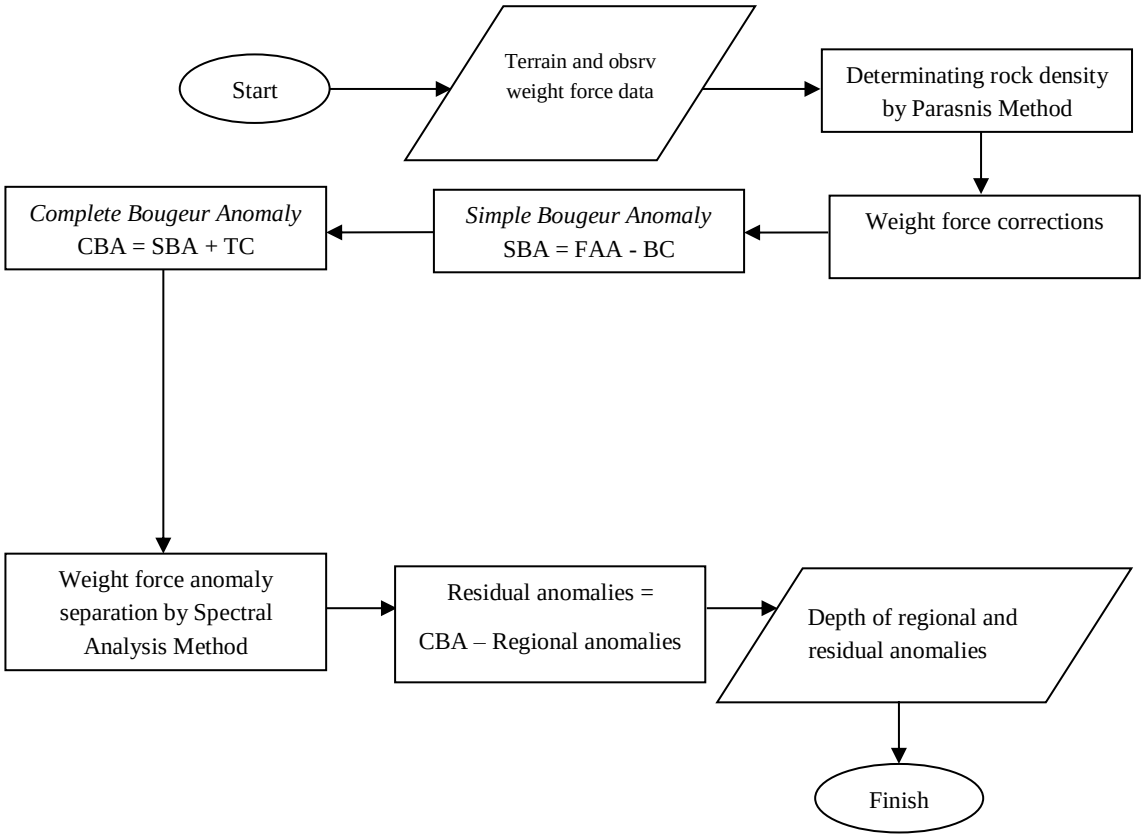

Figure 3. Flow chart

RESULTS AND DISCUSSION

The results of the ABL (Complete Bouger Anomaly) map in Figure 4 show that high anomalies between 86 mGall and 100 mGall are indicated by orange to red colors. Then the medium anomaly is indicated by green color which ranges from 70 mGall to 84 mGall. Low anomalies are indicated by purple to blue colors ranging from 54 mGall to 68 mGall. There are also 9 manifestations in the Way Ratai geothermal field that are illustrated by red triangle symbols.

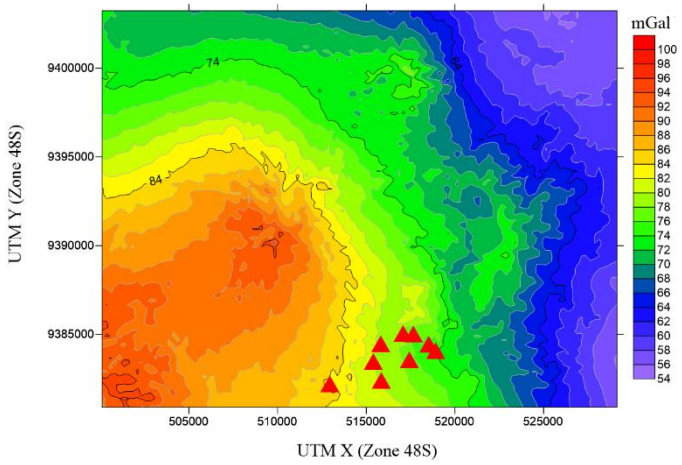

Figure 4. Complete Bouguer anomaly map with 2 mGal contour interval and red triangles indicating 9 manifestation points of the study area.

The complete Bouger anomaly obtained from the correction process is then made into 5 trajectories, namely A-A', B-B', C-C', D-D', and E-E' in Figure 5. This trajectory then becomes the input for separating regional and residual anomalies using the moving average method in Figure 6.

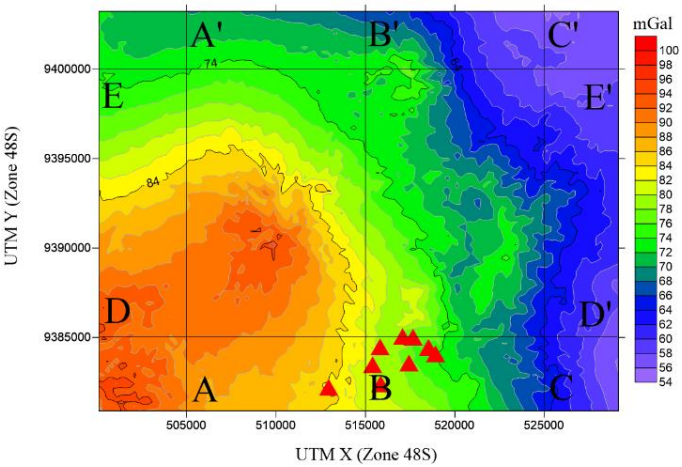

Figure 5. Lintasan *slice* analisis Spektrum dengan interval kontur 2 mGal dan segitiga merah menandakan 9 titik manifestasi daerah penelitian

(Figure 6) depicts the correlation graph between Ln A and K on track 1. There are two slopes of the line indicating regional and residual depth. Low values for the K parameter reflect data with low frequency, characterizing significant or regional depth. In contrast, relatively high values of K reflect data with high frequencies, indicating shallower or residual depths. In traverse 1, the estimated regional depth is 5322.2 meters and the residual depth is 351.39 meters. The boundary zone between regional and residual depths lies at a value of Kc (K cutoff) = 0.000771.

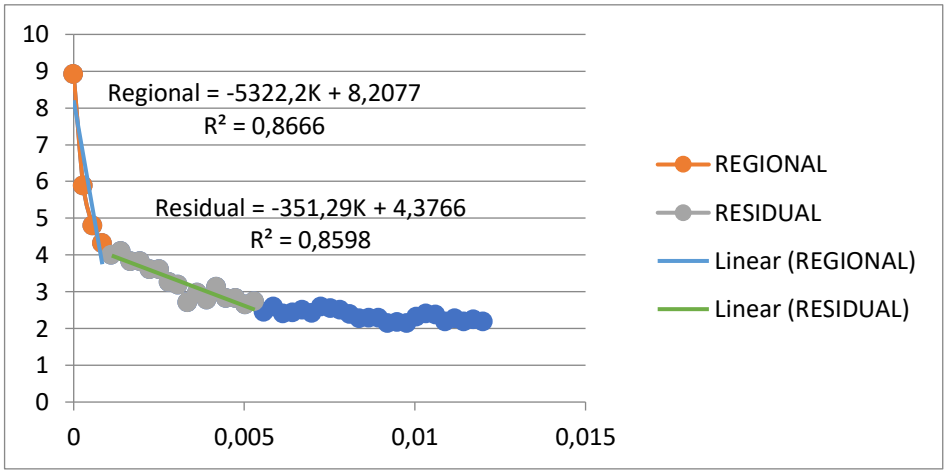

Figure 6. Ln A versus K curve of A-A' trajectory

(Figure 7) depicts the correlation graph between Ln A and K on track 2. There are two slopes of the line indicating regional and residual depth. Low values for the K parameter reflect data with low frequency, characterizing significant or regional depth. In contrast, relatively high values of K reflect high-frequency data, indicating shallower or residual depths. In traverse 2, the estimated regional depth is 5384.7 meters and the residual depth is 321.53 meters. The boundary zone between regional and residual depths lies at a value of Kc (K cutoff)=0.000762.

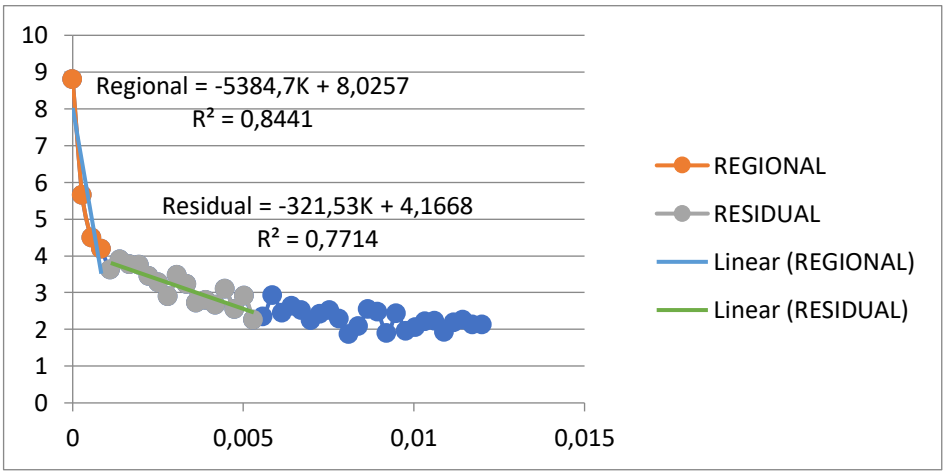

Figure 7. Ln A versus K curve of B-B' trajectory

(Figure 8) depicts the correlation graph between Ln A and K on track 3. There are two slope lines indicating regional and residual depth. Low values for the K parameter reflect data with low frequency, characterizing significant or regional depth. In contrast, relatively high values of K reflect high-frequency data, indicating shallower or residual depths. In traverse 3, the estimated regional depth is 5219.4 meters and the residual depth is 336.77 meters. The boundary zone between regional and residual depths lies at a value of Kc (K cutoff)=0.000855.

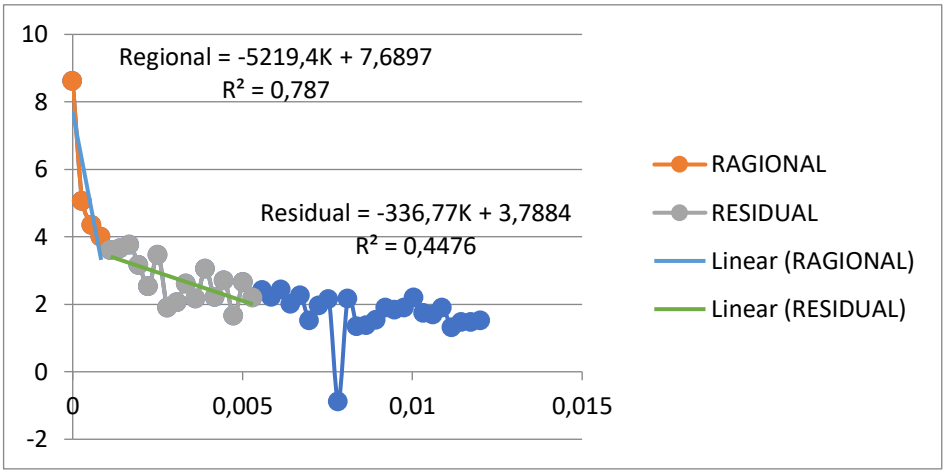

Figure 8. Ln A versus K curve of C-C' trajectory

(Figure 9) depicts the correlation graph between Ln A and K on track 4. There are two slopes of the line indicating regional and residual depth. Low values for the K parameter reflect data with low frequency, characterizing significant or regional depth. In contrast, relatively high values of K reflect high-frequency data, indicating shallower or residual depths. In traverse 4, the estimated regional depth is 4411.6 meters and the residual depth is 286.49 meters. The boundary zone between regional and residual depths lies at a value of Kc (K cutoff)=0.000829.

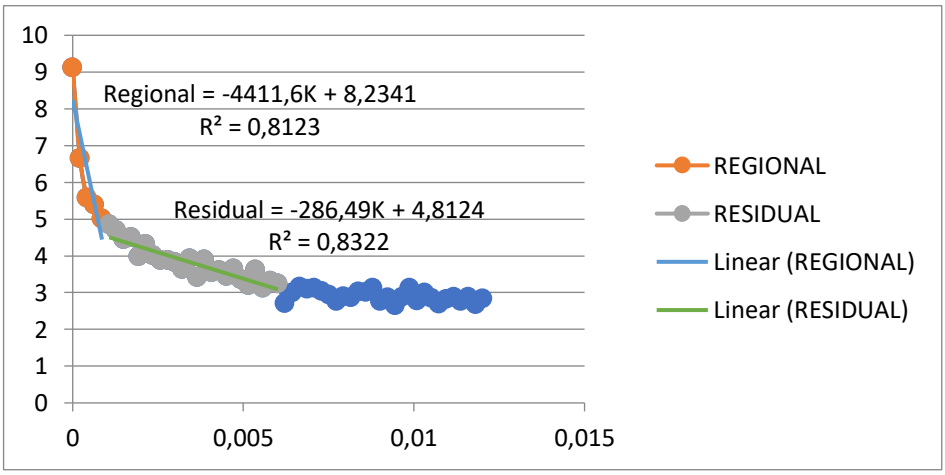

Figure 9. Ln A versus K curve of D-D' trajectory

(Figure 10) depicts the correlation graph between Ln A and K on track 5. There are two slopes of the line indicating regional and residual depth. Low values for the K parameter reflect data with low frequency, characterizing significant or regional depth. In contrast, relatively high values of K reflect high-frequency data, indicating shallower or residual depths. In traverse 5, the estimated regional depth is 5730.5 meters and the residual depth is 313.56 meters. The boundary zone between regional and residual depths lies at a value of Kc (K cutoff)=0.00077.

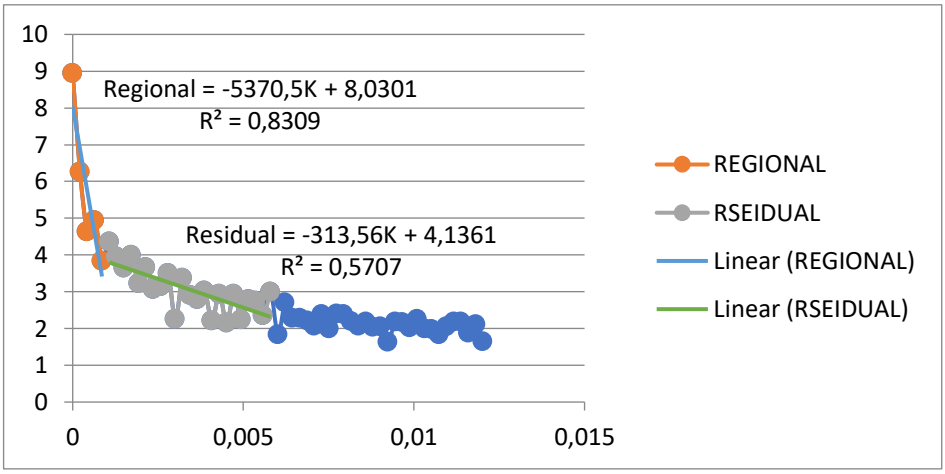

Figure 10. Ln A versus K curve of E-E' trajectory

From the five analyzed passes, the values of regional depth, residual depth, wave number, and window width were averaged.

Regional anomalies are gravity anomalies that show regional gravity anomalies in a study area. These anomalies are very deep and very wide. The regional anomaly in this study was obtained using a moving average filter with a window width of 33 from the complete Bouguer anomaly. It produced a regional anomaly map at a depth of 5213 meters. Regional anomalies in this study were obtained using a moving average filter where there are also 2 manifestations. With the highest anomaly value reaching 90 mGall and the lowest at 56 mGall as shown in (Figure 11).

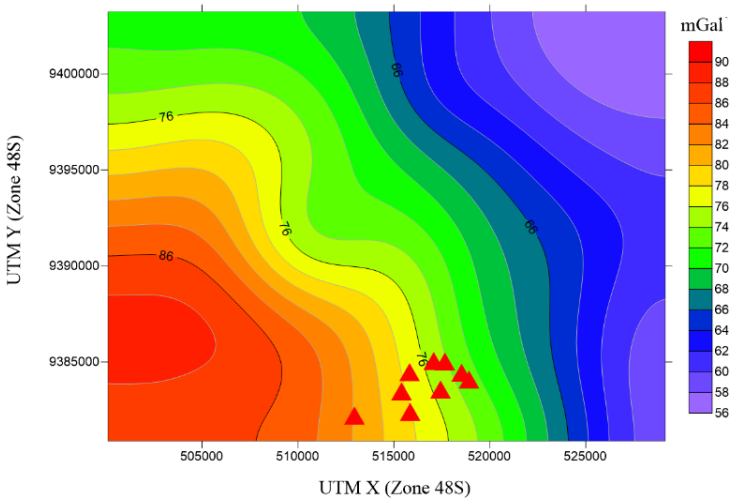

Figure 11. Regional Bouguer anomaly map with 2 mGal contour interval and red triangles indicate 9 manifestation points of the study area.

The residual anomaly map can be grouped into 3 groups based on the distribution of anomalies, namely the high anomaly group ranging from -3 mGall to 4 mGall and is usually colored red as in Figure 12. This high anomaly is usually caused by high igneous rock density and has not been altered, this rock is still fresh and massive. (Setiadi *et al*., 2014). Then the medium anomaly group that ranges from -11 mGall to -4 mGall is usually shown in green. Medium anomalies are caused by igneous rocks in the research location that have undergone alteration. The last anomaly is a group of low anomalies ranging from -19 mGall to -12 mGall which are usually marked in blue, according to the researchers (Zarkasyi *et al*., 2015). Low

anomalies are caused by rocks that have undergone a thorough alteration process which causes the rock density value to decrease.

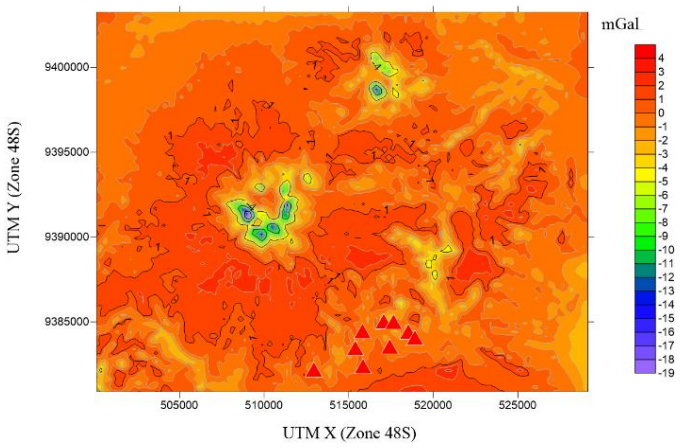

Figure 12. Residual Bouguer anomaly map with 2 mGal contour interval and red triangles indicate 9 manifestation points of the study area.

Separation of regional and residual anomalies through spectrum analysis produces values of regional depth, residual, wavelength, and cutoff value as the boundary of the intersection between regional and residual anomalies as in Table 1. Based on the anomaly separation graph on the A-A' track, the regional anomaly is obtained at a depth of 5322.2 m, the residual anomaly is at a depth of 351.29m. Based on the graph of the above analysis results on the B-B' track, the regional anomaly is obtained at a depth of 5384.7 m, and the residual anomaly is at a depth of 321.53 m. Based on the graph of the analysis results above on the C-C' track, the regional anomaly is obtained at a depth of 5219.4 m, and the residual anomaly is at a depth of 336.77 m. Based on the graph of the analysis results above on the D-D' track, the regional anomaly is obtained at a depth of 4411.6 m, and the residual anomaly is at a depth of 286.49 m.

Table 1. Regional-residual anomaly separation results, lambda, and K *cutoff*

Trajectory	Regional	Residual	N	Lambda (m)	K *cutoff* (cycle/m)
A-A’	5322.2	351.29	32.61	8152.528	0.000771
B-B’	5384.7	321.53	32.97	8244.017	0.000762
C-C’	5219.4	336.77	29.39	7347.562	0.000855
D-D’	4411.6	286.49	30.29	7574.48	0.000829
E-E’	5730.5	313.56	32.63	8159.654	0.00077
Average	5141.68	321.928	31.582	7895.648	0.000797

CONCLUSION

Spectrum analysis was conducted to separate the regional and residual anomalies. The depth of the regional anomaly obtained is 5213 m and the residual anomaly is 351.29 m. The range of regional anomaly values is 56 mGal to 90 mGal while the residual anomaly is in the range of -19 mGal to 4 mGal. Suggestions that can be given by the author are further research on the geothermal potential of Wayrtai and estimation in terms of economics for further

utilization.

REFERENCES

Blakely. (1995). *Potential Theory in Weight force and Magnetic Applications*. Cambridge University Press.

Charisma, P. A., Zarkasyi, A., Nandi Haerudin, dan, Teknik Geofisika, J., Teknik, F., Lampung, U., & Sumber Daya Mineral Batubara dan Panasbumi Bandung, P. (2022). Pemisahan Menggunakan Polynomial Fitting dan Analisis Second Vertical Derivative (SVD) untuk Mengidentifikasi Patahan pada Lapangan Panasbumi Pulau Pantar, Kabupaten Alor. *Jurnal Geologi Dan Sumberdaya Mineral*, *21*(2), 91–96. https://doi.org/10.33332/jgsm.geologi.v23.2.91-96

Donovan, R., Karyanto, K., & Dewanto, O. (2020). Studi Sifat Termal Batuan Daerah Lapangan Panas Bumi Way Ratai Berdasarkan Pengukuran Metode Konduktivitas Termal. *JGE (Jurnal Geofisika Eksplorasi)*, *4*(3), 325–340. https://doi.org/10.23960/jge.v4i3.44

Emujakporue, G. O. (2017). Subsurface temperature distribution from heat flow conduction equation in part of chad sedimentary basin, Nigeria. *Egyptian Journal of Petroleum*, *26*(2), 519–524. https://doi.org/10.1016/j.ejpe.2016.07.003

Fandari, A. El, Daryanto, A., & Suprayitno, G. (2014). Pengembangan Energi Panas Bumi yang Berkelanjutan. *Jurnal Ilmiah Semesta Teknika*, *17*(1), 68–82.

Hakim, A. F., Krismadiana, Sholihah, F., Ismawati, R., & Dewantari, N. (2022). Potensi dan Pemanfaatan Energi Panas Bumi di Indonesia. *Indonesian Journal of Conservation*, *11*(2), 71–77. https://doi.org/10.15294/ijc.v11i2.40599

Hidayat, N., & Basid, A. (2011). Analisis Anomali Gravitasi Sebagai Acuan dalam Penentuan Struktur Geologi Bawah Permukaan dan Potensi Geothermal. *Jurnal Neutrino*, *4*(1), 35–47.

Hirt, C., Claessens, S., Fecher, T., Kuhn, M., Pail, R., & Rexer, M. (2013). New ultrahigh-resolution picture of Earth's weight force field. *Geophysical Research Letters*, *40*(16), 4279–4283. https://doi.org/10.1002/grl.50838

Indriana, R. D., Brotopuspito, K. S., Setiawan, A., & Sunantyo, T. A. (2018). A Comparison Of Weight force Filtering Methods Using Wavelet Transformation And Moving Average (A Study Case Of Pre And Post Eruption Of Merapi In 2010 Yogyakarta, Indonesia). *IOSR Journal of Applied Geology and Geophysics*, *6*(3), 44–57. https://doi.org/10.9790/0990-0603024457

Karyanto, Haerudin, N., Mulyasari, R., Suharno, & Manurung, P. (2020). Geothermal potential assesment of way ratai area based on thermal conductivity measurement to measure thermal properties of rocks. *Journal of the Earth and Space Physics*, *45*(4), 89–98. https://doi.org/10.22059/jesphys.2020.267095.1007048

Karyanto, Haerudin, N., Zaenudin, A., Suharno, Darmawan, I. G. B., Adli, M., & Manurung, P. (2022). Numerical modeling for the steady-state condition of the geothermal system in way ratai. *Journal of Applied Science and Engineering (Taiwan)*, *25*(3), 447–456. https://doi.org/10.6180/jase.202206_25(3).0011

Khasmadin, M. F., & Harmoko, U. (2021). Kajian Potensi dan Pemanfaatan Energi Panas Bumi di Wilayah Kerja Panas Bumi Patuha Ciwidey. *Jurnal Energi Baru Dan Terbarukan*, *2*(2), 101–113. https://doi.org/10.14710/jebt.2021.11187

Mangga, S. A., Amirudin, T., Suwarti, Gafoer, S., & Sidarto. (1993). Peta Geologi Lembar Tanjungkarang, Sumatra. *Pusat Penelitian Dan Pengembangan Geologi*.

Marry, R. T., Armawi, A., Hadna, A. H., & Pitoyo, A. J. (2017). Panas Bumi Harta Karun Yang Terpendam Menuju Ketahanan Energi. *Jurnal Ketahanan Nasional*, *23*(2), 93. https://doi.org/10.22146/jkn.26944

Nurul, M., Yuliantina, A., Yulianata, A., Yogi, I. B. S., & Rasimeng, S. (2020). FORWARD MODELLING METODE GAYABERAT DENGAN MODEL INTRUSI DAN PATAHAN MENGGUNAKAN OCTAVE. *JURNAL GEOCELEBES*, *4*(2), 111–117. https://doi.org/10.20956/geocelebes.v4i2.10112

Nurwahyudin, D. S., & Harmoko, U. (2020). Pemanfaatan dan Arah Kebijakan Perencanaan Energi Panas Bumi di Indonesia Sebagai Keberlanjutan Maksimalisasi Energi Baru Terbarukan. *Jurnal Energi Baru Dan Terbarukan*, *1*(3), 111–123. https://doi.org/10.14710/jebt.2020.10032

Putri, M., Suharno, & Hidayatika, A. (2014). Introduction to Geothermal System of Way Ratai. *Proceedings Indonesia International Geothermal Convention & Exhibition*, 1–5. https://www.researchgate.net/publication/273444230

Raehanayati, Rachmansyah, A., & Maryanto, S. (2013). Studi Potensi Energi Geothermal Blawan-Ijen, Jawa Timur Berdasarkan Metode Weight force. *Jurnal Neutrino*, *6*(1), 31–39.

Sari, D. N. (2014). Pemodelan Weight force Kecamatan Dlingo Kabupaten Bantul Provinsi D.I. Yogyakarta. *Jurnal Ilmiah Pendidikan Fisika*, *3*(2).

Sarkowi. (2014). *Eksplorasi Gaya Berat*. Graha Ilmu.

Sarkowi, M., Wibowo, R. C., & Karyanto. (2021). Geothermal reservoir identification in way ratai area based on weight force data analysis. *Journal of Physics: Conference Series*, *2110*(1). https://doi.org/10.1088/1742-6596/2110/1/012004

Setiadi, I., Diyanti, A., & Ardi, N. D. (2014). Interpretasi Struktur Geologi Bawah Permukaan Daerah Leuwidamar Berdasarkan Analisis Spektral Data Gaya Berat. *Jurnal Geologi Dan Sumberdaya Mineral*, *15*(4), 205–214.

Sihombing, R. B., & Rustadi, R. (2020). Pemodelan dan Analisa Struktur Bawah Permukaan Daerah Prospek Panasbumi Kepahian Berdasarkan Metode Gayaberat. *JGE (Jurnal Geofisika Eksplorasi)*, *4*(2), 159–172. https://doi.org/10.23960/jge.v4i2.14

Siombone, S. H., Susilo, A., & Maryanto, S. (2022). Integration of Topex Satellite Weight force and DEM SRTM Imagery for Subsurface Structure Identification at Tiris Geothermal Area, Lamongan Volcano Complex, Probolinggo, East Java. *POSITRON*, *12*(2), 98. https://doi.org/10.26418/positron.v12i2.56880

Suharno. (2013). *Eksplorasi Geothermal*. Lembaga Penelitian Universitas Lampung.

Suprianto, A., Supriyadi, Priyantari, N., & Cahyono, B. E. (2021). Correlation between GGMPlus, topex and BGI weight force data in volcanic areas of Java Island. *Journal of Physics: Conference Series*, *1825*(1). https://doi.org/10.1088/1742-

6596/1825/1/012023

Supriyadi, Khumaedi, Sugiyanto, & Setiaswan, F. (2019). Pemisahan Anomali Regional dan Residual Data Gayaberat Studi Kasus di Kota Lama Semarang. *Physics Education Research Journal*, *1*(1), 29–36. https://ejournal.walisongo.ac.id/index.php/perj/index

Susilawati, A., Niode, M., Surmayadi, M., Pratomo, P. M., Nurhasan, Mustopa, E. J., Sutarno, D., & Srigutomo, W. (2023). Resistivity and Density Structure of Limboto Lake—Pentadio, Gorontalo, Indonesia Based on Magnetotelluric and Weight force Data. *Applied Sciences (Switzerland)*, *13*(1). https://doi.org/10.3390/app13010644

Telford, W. M., Geldart, L. P., & Sheriff, R. E. (1990). *Applied Geophysics* (2nd ed.). Cambridge University Press.

Wahyudi. (2006). Kajian Potensi Panas Bumi dan Rekomendasi Pemanfaatannya pada Daerah Prospek Gunungapi Ungaran Jawa Tengah (Geothermal Investigation and Its Application Recommendation in The Ungaran Geothermal Prospect Area, Central Java). *Berkala MIPA*, *16*(1), 41–48.

Zaenudin, A., Karyanto, Damayanti, L., & Sarkowi, M. (2011). Interpretasi Anomali Medan Magnetik pada Daerah Panasbumi Way Ratai Lampung. *The 11th Annual Indonesian Geothermal Association Meeting & Conference*.

Zakaria, M. F. (2021). Analisis Kedalaman Sumber Anomali Gravitasi menggunakan Spectral Statistical Technique di daerah Godean Yogyakarta. *Jurnal Fisika Flux: Jurnal Ilmiah Fisika FMIPA Universitas Lambung Mangkurat*, *18*(1), 75. https://doi.org/10.20527/flux.v18i1.8526

Zarkasyi, A., Supriyadi, Y., & Munandar, A. (2015). Survei Terpadu Gaya Berat dan Audiomagnetotellurik (AMT) Daerah Panas Bumi Pohon Batu, Kabupaten Seram Bagian Barat, Provinsi Maluku. *Prosiding Hasil Kegiatan Pusat Sumber Daya Geologi Tahun 2015*, 1–11.

Zuhdi, M., Ayub, S., Taufik, M., Syamsuddin, S., & Sukrisna, B. (2019). Moving Average Filter untuk Memisahkan Efek Dangkal Anomali Gravitasi Time Lapse. *Prisma Sains : Jurnal Pengkajian Ilmu Dan Pembelajaran Matematika Dan IPA IKIP Mataram*, *7*(2), 138. https://doi.org/10.33394/j-ps.v7i2.1766